Facile synthesis of ultrasmall PEGylated iron oxide nanoparticles for dual-contrast T_1- and T_2-weighted magnetic resonance imaging

2011 Nanotechnology 22 245604

(http://iopscience.iop.org/0957-4484/22/24/245604)

Nanotechnology **22** (2011) 245604 (7pp) doi:10.1088/0957-4484/22/24/245604

Facile synthesis of ultrasmall PEGylated iron oxide nanoparticles for dual-contrast T_1- and T_2-weighted magnetic resonance imaging

Fengqin Hu[1,3], Qiaojuan Jia[2], Yilin Li[2] and Mingyuan Gao[2]

[1] College of Chemistry, Beijing Normal University, Beijing 100875, People's Republic of China
[2] Institute of Chemistry, CAS, Bei Yi Jie 2, Beijing 100190, People's Republic of China

E-mail: fqhu@bnu.edu.cn

Received 7 January 2011, in final form 14 March 2011
Published 21 April 2011
Online at stacks.iop.org/Nano/22/245604

Abstract

The development of new types of high-performance nanoparticulate MR contrast agents with either positive (T_1) or dual-contrast (both positive and negative, $T_1 + T_2$) ability is of great importance. Here we report a facile synthesis of ultrasmall PEGylated iron oxide nanoparticles for dual-contrast T_1- and T_2-weighted MRI. The produced superparamagnetic iron oxide nanoparticles (SPIONs) are of high crystallinity and size uniformity with an average diameter of 5.4 nm, and can be individually dispersed in the physiological buffer with high stability. The SPIONs reveal an impressive saturation magnetization of 94 emu g^{-1} Fe_3O_4, the highest r_1 of 19.7 mM^{-1} s^{-1} and the lowest r_2/r_1 ratio of 2.0 at 1.5 T reported so far for PEGylated iron oxide nanoparticles. T_1- and T_2-weighted MR images showed that the SPIONs could not only improve surrounding water proton signals in the T_1-weighted image, but induce significant signal reduction in the T_2-weighted image. The good contrast effect of the SPIONs as $T_1 + T_2$ dual-contrast agents might be due to its high magnetization, optimal nanoparticle size for $T_1 + T_2$ dual-contrast agents, high size monodispersity and excellent colloidal stability. *In vitro* cell experiments showed that the SPIONs have little effect on HeLa cell viability.

S Online supplementary data available from stacks.iop.org/Nano/22/245604/mmedia

1. Introduction

Magnetic resonance imaging (MRI) is currently one of the most powerful tools for biological molecular imaging and clinical diagnosis [1–4]. One of the significant advantages of MRI is the ability to acquire three-dimensional tomographic information of whole tissue samples and animals with high spatial resolution and soft tissue contrast. In addition, images are acquired without the use of ionizing radiation or radiotracers. Medical diagnosis requires enhanced contrast between normal and pathological tissues, resulting in the development of exogenous MR contrast agents.

Most of the presently commercial MR contrast agents are paramagnetic molecular complexes, such as Gd^{3+} (seven unpaired electrons) and Mn^{2+} (five unpaired electrons) chelates, which are positive (T_1) contrast agents [5–7]. Their relaxivity ratio r_2/r_1 is commonly in the range of 1–2. Areas enriched with paramagnetic molecular complexes exhibit an increase in signal intensity and appear bright in T_1-weighted images [1, 5]. This kind of contrast agent is limited by their nonspecificity to target, quick removal by renal excretion and short accumulation time in practical applications [8].

Superparamagnetic nanoparticles (typically iron oxide nanoparticles) are another class of MR contrast agents that was normally used as negative (T_2) contrast agents. The nanoparticles commonly show a high r_2/r_1 ratio of at least 10, produce a decrease in signal intensity and appear dark in T_2-weighted images [9–16]. Compared with the conventional paramagnetic agents, nanoparticle-based contrast agents have

[3] Author to whom any correspondence should be addressed.

a number of advantages due to its nanoparticulate structures: (1) the magnetic properties of the agents can be tailored by size, shape, composition and assembly; (2) the nanoparticulate agents show tunable cellular uptake; (3) the agents have large specific surface areas that facilitate conjugation with targeting molecules and other probes for achieving targeting and multimodal agents and (4) the nanoscale dimension, adjustable surface structure and shape of the agents allow varying and favorable biodistribution. Nevertheless, a negative contrast effect and magnetic susceptibility artifacts are key factors that restrict the applications of superparamagnetic nanoparticles in MRI. The resulting dark signal might mislead the clinical diagnosis in T_2-weighted MRI because the signal is often confused with the signals from bleeding, calcification or metal deposits, and the susceptibility artifacts distort the background image [17, 18]. Therefore, the development of new types of nanoparticulate MR contrast agents with either T_1 or $T_1 + T_2$ dual-contrast ability is urgently needed.

For the above reasons, nanoparticles of Gd_2O_3 [19–22], GdF_3 [23], $GdPO_4$ [24] and MnO [18] have been investigated as T_1 MR contrast agents in the past few years. However, the sophisticated synthesis procedures and low r_1 values make them far from optimal for positive MRI. Recently, superparamagnetic iron oxide nanoparticles with ultrasmall sizes (<6 nm) were found to be good candidates for T_1 or $T_1 + T_2$ dual MR contrast agents [25–27]. Monodisperse ultrasmall iron oxide nanoparticles were mostly synthesized in non-polar organic solvents. They are only dispersible in non-polar organic solvents, and thus need surface modification with hydrophilic and biocompatible ligands before biomedical applications. For example, hydrophilic ultrasmall iron oxide nanoparticles with potential as T_1 contrast agents were synthesized through transferring hydrophobic nanoparticles by using tetramethylammonium hydroxide or phosphate-functionalized PEG [25, 26]. To avoid sophisticated phase transfer processes, the polyol method was utilized to synthesize ultrasmall water-dispersible iron oxide nanoparticles [27–29]. Nanoparticles prepared through this method can be dispersed in aqueous media and other polar solvents. In addition, the high reaction temperature favors nanoparticles with high crystallinity and monodispersity. A one-step synthesis of PEG-modified iron oxide nanoparticles with an average nanoparticle diameter of 1.7 nm has been developed [27]. Due to the small core size, the iron oxide nanoparticles have a low r_1 of 4.46 mM^{-1} s^{-1}. Recently, an approach was developed to synthesize water-dispersible iron oxide nanoparticles with a size range of 3–11 nm in diethylene glycol [28]. However, the poor colloidal stability of these nanoparticles at neutral pH makes them far from optimal for biomedical applications. Despite recent synthetic progress, it remains challenging to prepare monodisperse ultrasmall iron oxide nanoparticles with high r_1, low r_2/r_1 ratio and good colloidal stability under physiological conditions via a one-pot reaction [25–29] (see table S1 available at stacks.iop.org/Nano/22/245604/mmedia).

Herein, we present a facile synthesis of ultrasmall PEGylated iron oxide nanoparticles for dual-contrast T_1- and T_2-weighted MRI. Superparamagnetic iron oxide nanoparticles (SPIONs) with an average diameter of 5.4 nm were synthesized through decomposition of $Fe(acac)_3$ in triethylene glycol (TREG) in the presence of HOOC–PEG–COOH via a one-pot reaction. The produced SPIONs show excellent colloidal stability in the physiological buffer, present an impressive saturation magnetization of 94 emu g^{-1} Fe_3O_4 and a r_1 of 19.7 mM^{-1} s^{-1} as well as a r_2/r_1 ratio of 2.0 at 1.5 T. To the best of our knowledge, these are the highest r_1 and lowest r_2/r_1 ratio at 1.5 T reported so far for PEGylated iron oxide nanoparticles, indicating that the SPIONs are promising T_1+T_2 dual-contrast agents for a variety of MRI applications.

2. Experimental details

2.1. Synthesis of the SPIONs

Iron (III) acetylacetonate ($Fe(acac)_3$, 1.5 mmol, 99.9+%, Aldrich), poly(ethylene glycol) bis(carboxymethyl) ether (HOOC–PEG–COOH, 6 g, Aldrich, 600 g mol^{-1}) and triethylene glycol (TREG, 20 ml, 99%, Sigma-Aldrich) were mixed and purged with nitrogen. The reaction mixture was magnetically stirred at 100 °C until all of the reagents were completely dissolved in the solvent. Then, the temperature was increased to 260 °C and kept at that temperature for 30 min. After cooling to room temperature, the reaction solution was diluted five times by 0.1 M sodium citrate or 0.01 M phosphate buffer saline (PBS). Afterward, the SPIONs were collected by size filtration using Millipore Amicon Ultra 15 100 kDa centrifugal filters. The SPIONs were then redispersed in 0.1 M sodium citrate or 0.01 M PBS and collected by size filtration. After the dispersing and filtering procedures were repeated for six times, purified SPIONs were finally dispersed in 0.1 M sodium citrate or 0.01 M PBS for further investigation. A powder sample of the SPIONs for XRD and FTIR measurements was obtained by collecting the SPIONs through centrifugation of the reaction solution at 13 200 rpm for 30 min, washing with double-distilled water and ethanol for three times respectively, and then drying at room temperature.

2.2. Cell viability experiments

The colorimetric MTT assay was performed to determine the cytotoxicity of the SPIONs. Specifically, HeLa cells were first plated into a 96-well plate and cultured for about 24 h in Dulbecco's Modified Eagle Medium (DMEM, high glucose, GIBCO, C11995) supplemented with 10% fetal bovine serum (FBS, Thermo, SH3007003). Then, the cells were washed with PBS and incubated with 100 μl SPIONs at concentrations up to 500 μg Fe ml^{-1} at 37 °C for 24 h. Subsequently, the cells were washed twice with PBS followed by further culturing in the culture medium for 48 h. Afterwards, 20 μl of 5 mg ml^{-1} MTT (Amresco, 98%, code 0793) was added and allowed to react with the cells for 4 h before the addition of 150 μl DMSO (Amresco, code 0231) for dissolution of the precipitation. Finally, the absorption of each solution was measured at 490 nm on a SpectraMaxM5 microplate reader.

2.3. Characterization

TEM images and selected-area electron diffraction patterns were obtained on a JEM-2010 operated at an accelerating

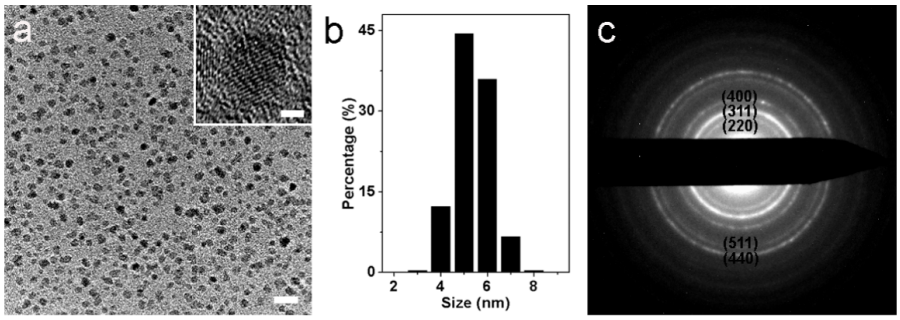

Figure 1. (a) TEM (inset is HR-TEM) images, (b) size distribution histogram and (c) electron diffraction patterns of the 5.4 nm SPIONs. The scale bar is 20 nm in the TEM image and 2 nm in the HR-TEM image.

voltage of 200 kV. HR-TEM images were obtained on a JEOL JEM-2100F FAST TEM operated at an accelerating voltage of 200 kV. Samples for TEM were prepared by spreading a drop of the solution sample on copper grids coated with a carbon film followed by evaporation under ambient conditions. XRD measurements were carried out on a powder sample of the SPIONs using a Regaku D/Max-2500 diffractometer. DLS measurements were performed with a Malvern Instruments Zetasizer Nano Series Nano-ZS. FTIR spectra were obtained with a Thermo Nicolet NEXUS 870 Fourier transform spectrometer. The transmission spectra of the SPIONs were taken after making pellets with KBr powder. A universal ATR sampling accessory was used to record the attenuated total reflection spectra of pure liquid TREG and HOOC–PEG–COOH (600 g mol^{-1}). Magnetic susceptibility measurements were carried out on a Quantum Design MPMS SQUID magnetometer. Samples were dispersed in 0.1 M sodium citrate and frozen under a nitrogen environment. Longitudinal and transverse relaxation times were measured at 1.5 T (60 MHz) and 37 °C on a Bruker mq60 NMR Analyzer. An inversion–recovery pulse sequence was used to measure the longitudinal relaxation times and a spin echo pulse sequence was used to measure the transverse relaxation times. MR phantom images were acquired on a Siemens 3 T TIM Trio clinical imaging system at ambient temperature (∼25 °C). A T_1-weighted image was acquired using a T_1-weighted spin echo pulse sequence with TR = 500 ms, TE = 11 ms, FOV = 75 × 100 mm^2, data matrix = 192 × 256, slice thickness = 2 mm and four signal averages. A T_2-weighted image was acquired using a T_2-weighted spin echo pulse sequence with TR = 1500 ms, TE = 75 ms, FOV = 75 × 100 mm^2, data matrix = 192 × 256, slice thickness = 2 mm and four signal averages. The iron concentration of each sample for SQUID and relaxivity was determined by inductively coupled plasma atomic emission spectroscopy (ICP-AES). Prior to ICP-AES measurements, the SPION samples were digested in ⩾69% *Trace*SELECT® nitric acid at 65 °C for ∼3 h and diluted to 3% (v/v) nitric acid.

3. Results and discussion

A polyol process was designed to synthesize SPIONs by using $Fe(acac)_3$ as the iron precursor, HOOC–PEG–COOH as the stabilizer and TREG as the solvent and reducing agent. Typically, 5.4 nm SPIONs were prepared by heating a mixture of 1.5 mmol $Fe(acac)_3$, 6 g HOOC–PEG–COOH (600 g mol^{-1}) and 20 ml TREG at 260 °C for 30 min. Figure 1(a) shows the representative TEM and HR-TEM images of the SPIONs. The histogram of the nanoparticle size based on statistical results is shown in figure 1(b). The average nanoparticle size is 5.4 nm. A standard deviation of 0.7 nm demonstrates the high monodispersity of the SPIONs prepared with this procedure. Selected-area electron diffraction patterns shown in figure 1(c) reveal that the SPIONs are of high crystallinity. The lattice spacings (calculated on the basis of the diffraction patterns) are in agreement with those of a bulk inverse spinel iron oxide such as magnetite (JCPDS 19-0629, Fe_3O_4) or maghemite (JCPDS 39-1346, γ-Fe_2O_3). The crystal structure was also investigated by powder x-ray diffraction (XRD). As shown in figure 2, the position and relative intensity of the strong diffraction peaks of the SPIONs correspond to a cubic structure of the inverse spinel iron oxide. The average particle size calculated with Debye–Scherrer's formula is 5.1 nm, which is quite close to the TEM result. Note that, it is very difficult to distinguish between these two spinel structures (magnetite and maghemite) with selected-area electron diffraction and XRD patterns. The chemical composition of the SPIONs will be demonstrated in the following FTIR spectra.

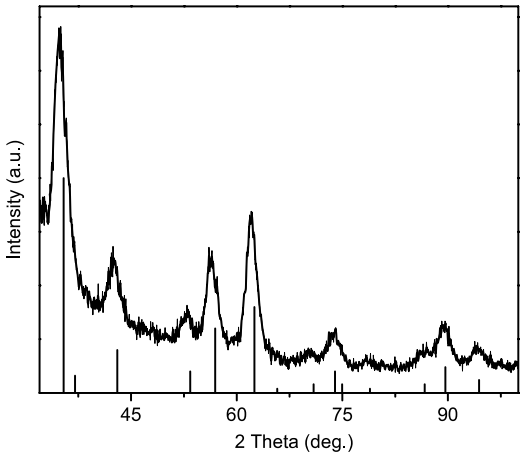

Figure 2. Powder x-ray diffractogram of the 5.4 nm SPIONs. Bottom: JCPDS card (19-0629) data for magnetite.

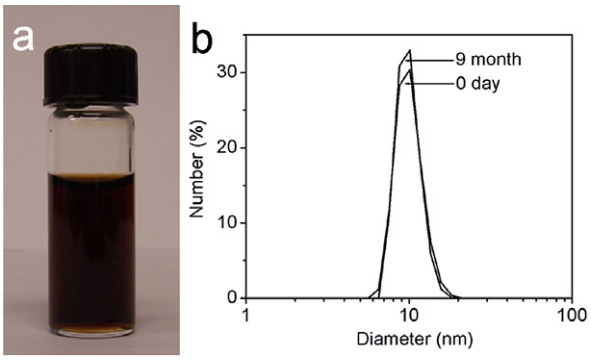

Figure 3. (a) Photograph of PBS suspension of the 5.4 nm SPIONs after placement for 9 months at room temperature. (b) Hydrodynamic size distributions of the 5.4 nm SPIONs freshly dispersed in PBS and after placement for 9 months measured with DLS.

(This figure is in colour only in the electronic version)

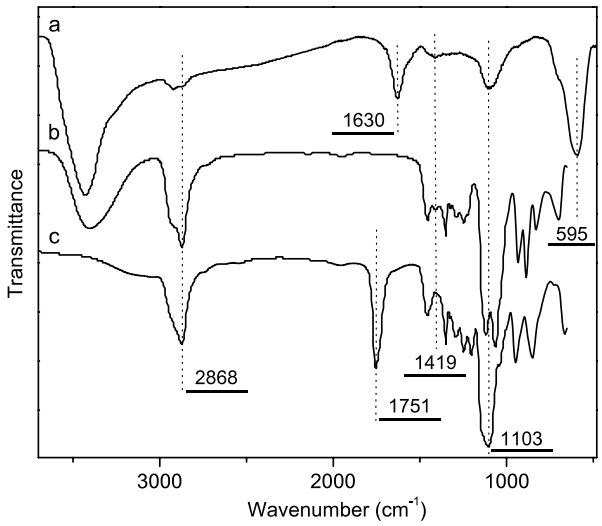

Figure 4. FTIR spectra of (a) the 5.4 nm SPIONs, (b) TREG and (c) HOOC–PEG–COOH.

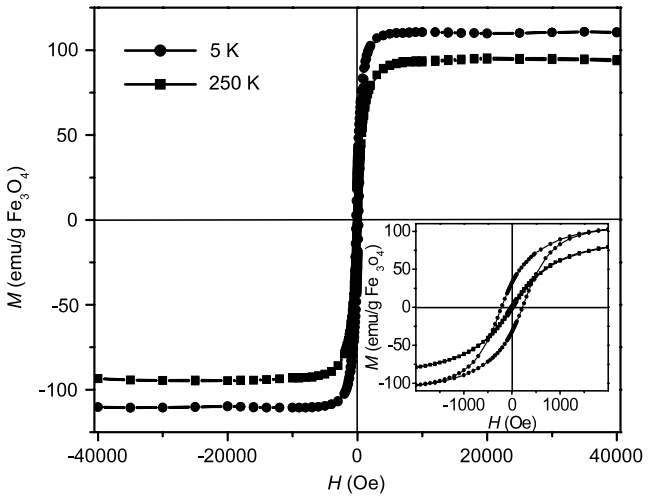

Figure 5. Magnetization (M) loops for the 5.4 nm SPIONs measured at 5 and 250 K. The inset shows an expanded view of the low magnetic field behavior for both temperatures.

The polyol method possesses both merits of the syntheses in non-polar organic solvent and in aqueous solvent. The former provides a monodisperse particle diameter, whereas the latter provides an easy synthesis for water solubility and biocompatibility. As expected, the 5.4 nm SPIONs showed high monodispersity with a standard deviation of 0.7 nm, and can be readily dispersed in aqueous media without any further surface modification. The SPIONs can also form a stable dispersion in PBS at the same pH value and ionic strength as physiological conditions. This colloid remains stable at room temperature for several months without noticeable precipitation, as shown in figure 3(a). The colloidal stability of the SPIONs was further investigated through dynamic light scattering (DLS). As shown in figure 3(b), the hydrodynamic diameter of the SPIONs freshly dispersed in PBS is 10.1 nm, which remains unchanged after placement of the solution for 9 months. This indicates that the SPIONs prepared with the current procedure show excellent colloidal stability in PBS, which is promising for *in vitro* and *in vivo* biomedical applications.

The surface chemical structure of the SPIONs was characterized by Fourier transform infrared (FTIR) spectroscopy. The FTIR spectra of the SPIONs, TREG and HOOC–PEG–COOH were shown in figure 4. The characteristic bands of HOOC–PEG–COOH at 1103 cm^{-1} (C–O–C stretch) and 2868 cm^{-1} (CH_2 stretch) appear in the spectrum of the SPIONs, indicating that HOOC–PEG–COOH is present on the SPION nanocrystal surfaces. The distinct spectral difference between HOOC–PEG–COOH and the SPIONs is that the carboxyl band at 1751 cm^{-1} for HOOC–PEG–COOH is shifted to a lower wavenumber, 1630 cm^{-1}, accompanied by the appearance of a new band at 1419 cm^{-1} in the spectrum of the SPIONs. This spectral change indicates that the carboxylate group interacts with the iron on the SPION surface [30]. In addition, the spectrum of the SPIONs exhibits characteristic peaks centered at 595 cm^{-1} that are attributed to lattice absorption of the SPIONs [31–33]. It has been demonstrated that magnetite and maghemite can be identified from each other through their lattice absorption peaks in the FTIR spectra. The lattice adsorption peaks of the SPIONs centered at 595 cm^{-1} indicate that the SPIONs are probably magnetite [33, 34]. After the PEG-coated SPIONs were dispersed in sodium citrate or PBS, both FTIR spectra and colloidal stability suggest that citrate or phosphate has been modified on the SPION surfaces even though PEG is still the primary surface coating ligand (figure S1 available at stacks.iop.org/Nano/22/245604/mmedia).

The magnetic properties of the SPIONs were measured using a superconducting quantum interference device (SQUID). Figure 5 shows the magnetization loops measured at 5 and 250 K. At 250 K, the SPIONs exhibit superparamagnetic behavior without magnetic hysteresis and remanence, whereas ferromagnetic behavior with a coercivity of 220 Oe is observed at 5 K since thermal energy is insufficient to induce moment randomization. The saturation magnetization of the SPIONs at 250 K is 94 emu $g^{-1}Fe_3O_4$, which is close to the value of bulk magnetite (98 emu g^{-1}). This value is quite impressive and well above the ones reported previously [29, 35]. The

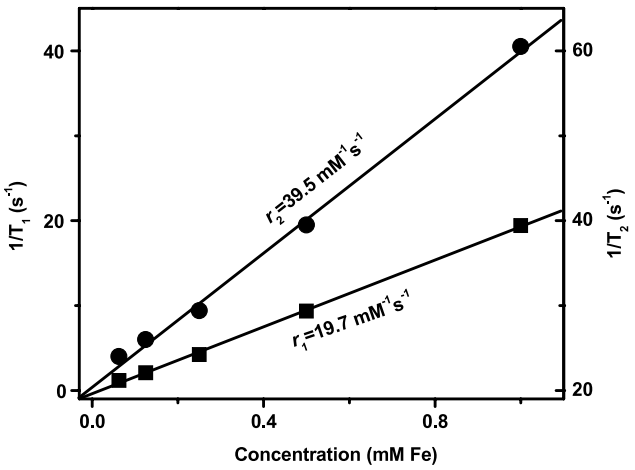

Figure 6. T_1 and T_2 relaxation rates ($1/T_{1,2}$) plotted against the Fe concentrations of the 5.4 nm SPIONs (1.5 T, 37 °C).

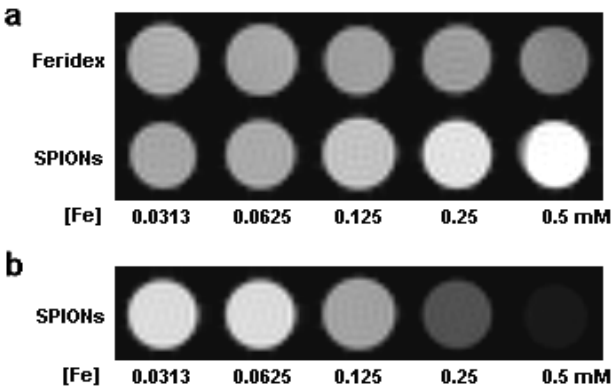

Figure 7. (a) T_1-weighted and (b) T_2-weighted MR images of aqueous solutions of commercial Feridex and the 5.4 nm SPIONs at different Fe concentrations.

higher the saturation magnetization is, the more important is the material for practical applications. The high saturation magnetization value found in the SPIONs might be related to the high crystallinity of the SPIONs and the nature of the surface coating material (HOOC–PEG–COOH) used. It was demonstrated that acids can decrease the spin disorder at the surface of the nanoparticles and enhance the saturation magnetization value. This kind of behavior has also been observed in Fe_3O_4 nanoparticles coated with oleic acid [36].

$T_1 + T_2$ dual-contrast agents require a high r_1 and a r_2 which is not significantly larger than r_1. The use of iron oxide nanoparticles as $T_1 + T_2$ dual-contrast agents is, in most cases, limited due to the large r_2/r_1 ratio although the r_1 is often higher compared to paramagnetic chelates. Therefore, to achieve the successful use of iron oxide nanoparticles in dual-contrast T_1- and T_2-weighted MRI, one should try to maximize r_1 while keeping r_2 as small as possible. MR measurements were performed in order to investigate the ability of the SPIONs to shorten the T_1 and T_2 and thus evaluate whether it is suitable as $T_1 + T_2$ dual-contrast agents. T_1 and T_2 of the SPIONs at different Fe concentrations were measured on a 1.5 T (60 MHz) relaxometer at 37 °C. The r_1 and r_2 of the SPIONs were determined by calculating the slope of a plot of $1/T_1$ and $1/T_2$ versus Fe concentration. As shown in figure 6, the r_1 and r_2 of the SPIONs are 19.7 and 39.5 $mM^{-1}\ s^{-1}$, respectively. Therefore, the r_2/r_1 ratio of the as-developed contrast agents is 2.0. These are the highest r_1 and lowest r_2/r_1 ratios at 1.5 T reported so far for PEGylated iron oxide nanoparticles (see table S1 available at stacks.iop.org/Nano/22/245604/mmedia). It is worth noting that the r_1 of the SPIONs is 1.7 times higher than that of the recently reported PEG-coated Fe_3O_4 T_1 contrast agents (7.3 $mM^{-1}\ s^{-1}$, 1.5 T) and even 4.5 times higher than that of magnevist (3.6 $mM^{-1}\ s^{-1}$, 1.5 T), which is a typical T_1 contrast agent based on gadolinium as a clinical standard [26]. The high r_1 as well as low r_2/r_1 ratio makes the as-developed SPIONs an ideal candidate for $T_1 + T_2$ dual-contrast agents at clinically relevant magnetic fields.

To further validate the potential of the SPIONs as $T_1 + T_2$ dual-contrast agents, we acquired T_1- and T_2-weighted MR images as a function of iron concentration using a 3.0 T MRI scanner. As shown in figure 7, the SPIONs induced a bright signal enhancement in a concentration-dependent manner in the T_1-weighted MR image. Compared to a commercially available Feridex, which is also an iron oxide nanoparticle-based contrast agent, the SPIONs exhibited much better T_1 positive contrast. In the T_2-weighted MR image, the SPIONs also displayed a significant signal reduction with increasing nanoparticle concentration. The MR images indicate that the SPIONs could be utilized as high-performance $T_1 + T_2$ dual-contrast agents.

The high saturation magnetization (94 emu $g^{-1}Fe_3O_4$) of the SPIONs is a factor in its high r_1 value [25]. Optimal core size with good monodispersity is also very important for nanoparticulate $T_1 + T_2$ dual-contrast agents: it should be both large enough to offer a high r_1, and small and monodisperse enough to cause a small r_2/r_1 ratio [37]. It has been suggested that a core size of approximately 5 nm is optimal to form a $T_1 + T_2$ dual-contrast agent based on iron oxide nanoparticles [26]. Besides nanoparticle size, size uniformity also affects the r_2/r_1 ratio of the magnetic nanoparticles. An increase of nanoparticle size leads to an increase in both r_1 and r_2. However, this effect on r_2 is much more significant than that on r_1. Therefore, a small increase of nanoparticle size results in a large increase of r_2/r_1 ratio. Therefore, high monodispersity of nanoparticle size is desired for $T_1 + T_2$ dual-contrast agents. The SPIONs we produced are with the optimal diameter of 5.4 nm and high size monodispersity (SD = 0.7 nm), resulting in its high r_1 and low r_2/r_1 ratio.

Excluding aggregation of magnetic nanoparticles is essential to obtain high-performance $T_1 + T_2$ dual-contrast agents since the transverse relaxation effect is enhanced while T_1-shortening is weakened when agglomeration occurs [38]. So far, a lot of work has been done on the use of PEG as a ligand for iron oxide nanocrystals [39, 40]. However, the coating of nanoparticles with PEG often results in large hydrodynamic diameters and the formation of small amounts of aggregates, which in turn enables these systems to act as T_2 while not as T_1 contrast agents. In this work, the hydrodynamic diameter of the 5.4 nm SPIONs is 10.1 nm, which is slightly larger than the superposition of an iron oxide core and PEG

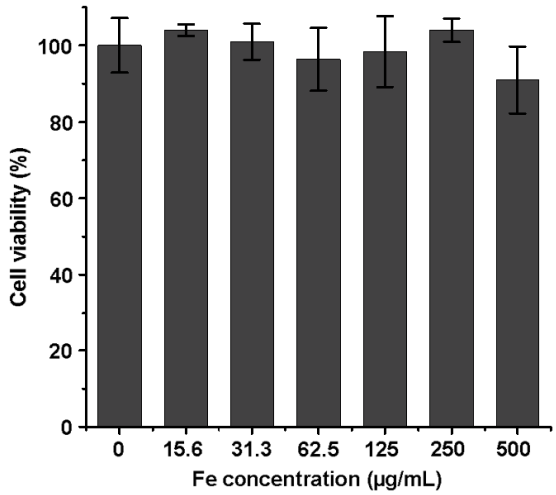

Figure 8. Viability of HeLa cells after 24 h incubation with the 5.4 nm SPIONs at various Fe incubation concentrations.

coating since counterions and water form a diffuse layer which moves with the SPIONs. This indicates that the SPIONs are individually dispersed. Furthermore, the hydrodynamic diameter of the SPIONs has excellent stability during the 9 month measurement period. The excellent dispersity of the SPIONs in aqueous solution could be another factor for its high r_1 and low r_2/r_1 ratio.

The cytotoxicity of the SPIONs was determined using the colorimetric MTT assay on HeLa cells. For this study, HeLa cells were incubated with 15.6, 31.3, 62.5, 125, 250 or 500 μg Fe ml^{-1} of the SPIONs for 24 h. As shown in figure 8, after 24 h incubation, the viability of HeLa cells was still >90% at all Fe incubation concentrations. These results demonstrate that the SPIONs show little cytotoxicity, indicating that they have potential in *in vivo* MRI applications.

4. Conclusions

In summary, a facile one-pot reaction was developed to synthesize 5.4 nm water-soluble PEG-coated SPIONs which can act as high-performance $T_1 + T_2$ dual MR contrast agents. The SPIONs produced with this procedure are highly crystalline, superparamagnetic at room temperature, and can be individually dispersed in the physiological buffer with high stability. The SPIONs present an impressive saturation magnetization value of 94 emu g^{-1} Fe_3O_4 and a r_1 of 19.7 mM^{-1} s^{-1} as well as a r_2/r_1 ratio of 2.0 at 1.5 T. T_1- and T_2-weighted MR images demonstrated that the SPIONs could be utilized as high-performance $T_1 + T_2$ dual-contrast agents. High magnetization, optimal nanoparticle size for $T_1 + T_2$ dual-contrast agents, high size monodispersity and excellent colloidal stability might be factors for the good contrast effect of the SPIONs as $T_1 + T_2$ dual-contrast agents. The cell viability assay showed that the SPIONs have little effect on HeLa cell viability. The novel SPIONs should have great potential in dual-contrast T_1- and T_2-weighted MRI for molecular imaging and diagnostic applications.

Acknowledgments

This work was supported by the initial funding of science research from the College of Chemistry, Beijing Normal University, the Fundamental Research Funds for the Central Universities, and the Youth Science Foundation of Beijing Normal University (no. 105501GK).

References

[1] Merbach A E and Toth E 2001 *The Chemistry of Contrast Agents in Medical Magnetic Resonance Imaging* (New York: Wiley)
[2] Aime S, Cabella C, Colombatto S, Geninatti Crich S, Gianolio E and Maggioni F 2002 *J. Magn. Reson. Imag.* **16** 394–406
[3] Hu X and Norris D G 2004 *Annu. Rev. Biomed. Eng.* **6** 157–84
[4] Winter Patrick M, Caruthers Shelton D, Wickline Samuel A and Lanza Gregory M 2006 *Curr. Cardiol. Rep.* **8** 65–9
[5] Caravan P, Ellison J J, McMurry T J and Lauffer R B 1999 *Chem. Rev.* **99** 2293–352
[6] Major J L and Meade T J 2009 *Acc. Chem. Res.* **42** 893–903
[7] Shu C Y *et al* 2009 *Bioconjug. Chem.* **20** 1186–93
[8] Morawski A M, Lanza G A and Wickline S A 2005 *Curr. Opin. Biotechnol.* **16** 89–92
[9] Taboada E, Solanas R, Rodriguez E, Weissleder R and Roig A 2009 *Adv. Funct. Mater.* **19** 2319–24
[10] Mendonca Dias M H and Lauterbur P C 1986 *Magn. Reson. Med.* **3** 328–30
[11] Semelka R C and Helmberger T K G 2001 *Radiology* **218** 27–38
[12] Qiao R R, Yang C H and Gao M Y 2009 *J. Mater. Chem.* **19** 6274–93
[13] Hu F Q, Wei L, Zhou Z, Ran Y L, Li Z and Gao M Y 2006 *Adv. Mater.* **18** 2553–6
[14] Li Z, Wei L, Gao M Y and Lei H 2005 *Adv. Mater.* **17** 1001–5
[15] Sun C, Lee J S H and Zhang M Q 2008 *Adv. Drug Deliv. Rev.* **60** 1252–65
[16] Maity D, Chandrasekharan P, Yang C-T, Chuang K-H, Shuter B, Xue J-M, Ding J and Feng S-S 2010 *Nanomedicine* **5** 1571–84
[17] Bulte J W M and Kraitchman D L 2004 *NMR Biomed.* **17** 484–99
[18] Na H B *et al* 2007 *Angew. Chem. Int. Edn* **46** 5397–401
[19] McDonald M A and Watkin K L 2006 *Acad. Radiol.* **13** 421–7
[20] Fortin M A, Petoral R M, Soderlind F, Klasson A, Engstrom M, Veres T, Kall P O and Uvdal K 2007 *Nanotechnology* **18** 395501
[21] Bridot J L *et al* 2007 *J. Am. Chem. Soc.* **129** 5076–84
[22] Park J Y, Baek M J, Choi E S, Woo S, Kim J H, Kim T J, Jung J C, Chae K S, Chang Y and Lee G H 2009 *ACS Nano* **3** 3663–9
[23] Evanics F, Diamente P R, van Veggel F, Stanisz G J and Prosser R S 2006 *Chem. Mater.* **18** 2499–505
[24] Hifumi H, Yamaoka S, Tanimoto A, Citterio D and Suzuki K 2006 *J. Am. Chem. Soc.* **128** 15090–1
[25] Taboada E, Rodriguez E, Roig A, Oro J, Roch A and Muller R N 2007 *Langmuir* **23** 4583–8
[26] Tromsdorf U I, Bruns O T, Salmen S C, Beisiegel U and Weller H 2009 *Nano Lett.* **9** 4434–40
[27] Park J Y, Daksha P, Lee G H, Woo S and Chang Y M 2008 *Nanotechnology* **19** 365603
[28] Jia X, Chen D R, Jiao X L and Zhai S M 2009 *Chem. Commun.* **8** 968–70
[29] Hu F Q, MacRenaris K W, Waters E A, Liang T Y, Schultz-Sikma E A, Eckermann A L and Meade T J 2009 *J. Phys. Chem.* C **113** 20855–60

[30] Liu Q and Xu Z 1995 *Langmuir* **11** 4617–22
[31] Jun Y W *et al* 2005 *J. Am. Chem. Soc.* **127** 5732–3
[32] Hu F Q, Li Z, Tu C F and Gao M Y 2007 *J. Colloid Interface Sci.* **311** 469–74
[33] Tartaj P, Morales M D, Veintemillas-Verdaguer S, Gonzalez-Carreno T and Serna C J 2003 *J. Phys. D: Appl. Phys.* **36** R182–97
[34] Daou T J, Greneche J M, Pourroy G, Buathong S, Derory A, Ulhaq-Bouillet C, Donnio B, Guillon D and Begin-Colin S 2008 *Chem. Mater.* **20** 5869–75
[35] Li Z, Chen H, Bao H B and Gao M Y 2004 *Chem. Mater.* **16** 1391–3
[36] Guardia P, Batlle-Brugal B, Roca A G, Iglesias O, Morales M P, Serna C J, Labarta A and Batlle X 2007 *J. Magn. Magn. Mater.* **316** E756–9
[37] Kellar K E, Fujii D K, Gunther W H H, Briley-Saebo K, Bjornerud A, Spiller M and Koenig S H 2000 *J. Magn. Reson. Imag.* **11** 488–94
[38] Roch A, Gossuin Y, Muller R N and Gillis P 2005 *J. Magn. Magn. Mater.* **293** 532–9
[39] Xie J, Xu C J, Xu Z C, Hou Y L, Young K L, Wang S X, Pourmond N and Sun S H 2006 *Chem. Mater.* **18** 5401–3
[40] Xie J, Xu C J, Kohler N, Hou Y L and Sun S H 2007 *Adv. Mater.* **19** 3163–6